Journal of Colloid and Interface Science 391 (2013) 158–167

Contents lists available at SciVerse ScienceDirect

Journal of Colloid and Interface Science

www.elsevier.com/locate/jcis

A direct surface modification of iron oxide nanoparticles with various poly(amino acid)s for use as magnetic resonance probes

Hee-Man Yang [a], Chan Woo Park [b], Taebin Ahn [b], Bokyung Jung [b], Bum-Kyoung Seo [a], Jung-Hwan Park [c], Jong-Duk Kim [b,*]

[a] Decontamination & Decommissioning Research Division, Korea Atomic Energy Research Institute, Daejeon 305-353, Republic of Korea
[b] Department of Chemical and Biomolecular Engineering (BK21 Graduate Program), Korea Advanced Institute of Science and Technology, Daejeon 305-701, Republic of Korea
[c] Department of Bionano Technology, Gacheon BioNano Research Institute, Kyungwon University, Seongnam, Gyeonggi-Do 461-701, Republic of Korea

ARTICLE INFO

Article history:
Received 27 June 2012
Accepted 19 September 2012
Available online 8 October 2012

Keywords:
Poly(amino acid)s
Iron oxide nanoparticles
Surface modification
Magnetic resonance probes

ABSTRACT

Water soluble and biocompatible iron oxide nanoparticles coated with poly(aspartic acid) (PAsp), poly(asparagines) (PAsn), poly(2-hydroxy-ethyl L-aspartamide) (PHEA), and poly-α,β-(*N*-2-dimethylaminoethyl L-aspartamide) (PDMAEA) were prepared by hydrophobic interaction between hydrophobic iron oxide nanoparticles and each amphiphilic poly(amino acid)s graft polymer. The octadecyl side chain grafted poly(succinimide)(PSI-*g*-C_{18}), used as a precursor polymer, was easily aminolyzed with nucleophilic compounds to form various poly(amino acid)s graft polymer (PAsp-*g*-C_{18}, PAsn-*g*-C_{18}, PHEA-*g*-C_{18}, PDMAEA-*g*-C_{18},) and simultaneously stabilize the dispersion of iron oxide nanoparticles in aqueous solution. The diameters of the poly(amino acid)s coated iron oxide nanoparticles (PAIONs) were smaller than 30 nm in aqueous solution, extremely stable in aqueous solutions with a wide range of pH and salt concentrations. Further, all the PAIONs showed excellent MR signal intensities (high r_2 values) and the cellular uptake property of the PAIONs was also evaluated.

1. Introduction

Superparamagnetic iron oxide nanoparticles have received attention in the biomedical field for medical imaging, drug delivery, cell and protein separation, and magnetic cellular labeling [1–3]. In particular, iron oxide nanoparticles (Fe_3O_4 and γ-Fe_2O_3) synthesized by thermal decomposition methods have been widely used because of their high crystallinity and monodispersed size distribution [4–6]. However, the stabilized iron oxide nanoparticles are only soluble in organic solvents due to the hydrophobic alkyl ligands on the nanoparticles surface [7,8]. Surface modification of these nanopartilces is essential to render their surface hydrophilic and maintain the dispersion stable under physiological conditions [9,10]. The size and surface properties of iron oxide nanoparticles are important parameter for an in vivo magnetic resonance imaging (MRI) application. In general, nanoparticles of a hydrodynamic size smaller than 40 nm can escape from the non-specific uptake by a reticular-endothelial system (RES) more easily than those of larger than 40 nm [2,7]. In addition, positively charged nanoparticles would be cleared in the blood circulation in a body by the absorption of plasma proteins (opsonization) [11,12], but negatively charged nanoparticles have a high resistance against opsonization [13] However, positively charged nanoparticles have a higher adsorption affinity at negatively charged cell membranes than negatively charged nanoparticles do [14].

Recently, various methods have been reported for the surface modification of hydrophobically stabilized iron oxide nanoparticles [15–25]. Poly(ethylene glycol)(PEG) are widely used as shell materials because of their attractive advantages such as biocompatibility, diminished non-specific uptake by RES and prolonged blood circulation time [17–23]. However, some studies reported that PEG may possess antigenic, immunogenic properties and accelerated blood clearance phenomenon [26–28].

Biocompatible and biodegradable poly(α-amino acid)s and their derivatives synthesized from poly(succinimide) can be excellent alternative materials and are already widely investigated as drug delivery carriers [29–34] because of their biodegradability by proteloytic enzymes [35,36]. Poly(α-amino acid)s have many attractive properties such as absence of toxicity, antigenicity, and immunogenicity [37]. In particular, carboxylic group of PAsp can attach the small molecules such as drug and targeting moiety. PHEA coated liposome results in significantly prolonged blood circulation times over those of non-coated and PEG coated liposomes [38]. Dimethylaminoethyl group of PDMAEA is widely used as a functional moiety in many polymethacrylate-based drug delivery

* Corresponding author. Fax: +82 42 350 3910.
E-mail address: kjd@kaist.ac.kr (J.-D. Kim).

0021-9797/$ - see front matter Crown Copyright © 2012 Published by Elsevier Inc. All rights reserved.
http://dx.doi.org/10.1016/j.jcis.2012.09.044

carriers for gene delivery and stimuli-sensitive drug delivery. Recently, our group reported the synthesis and application of poly(amino acid)s derivatives, PHEA, coated iron oxide nanoparticles with hydrodynamic size smaller than 40 nm through dual interaction [39,40]. However, the surface modification method was multistep procedure and could not control the polymer shell of nanoparticles because only PHEA was soluble and succeeded in coating the nanoparticles in the reaction mixture. Thus, a more simplified and shell controllable coating procedure is still desired.

The present study investigates simplified surface modification of iron oxide nanoparticles with different poly(amino acid)s, namely, PAsp-, PAsn-, PHEA-, and PDMAEA. Different poly(amino acid) shell were synthesized from a same precursor polymer, octedecyl side chain grafted poly(succinimide), by reaction with different nucleophilic compounds in aqueous solutions and simultaneously coated the hydrophobic nanoparticles with each amphipihlic poly(amino acid)s via hydrophobic interaction for phase transfer of nanoparticles from organic to aqueous phases. This is a very simple and convenient way to synthesize water soluble and biocompatible iron oxide nanoparticels having different surface properties and a hydrodynamic size smaller than 30 nm.

2. Materials and methods

2.1. Materials

Iron (III) acetylacetonate, benzyl ether, oleic acid (90%), oleylamine (>70%), 1,2-hexadecanediol (90%), L-aspartic acid, mesitylene, sulfolane, aminoethanol, octadecylamine, tetrahydrofuran, sodium hydroxide, ammonium hydroxide were purchased from Sigma–Aldrich and were used as received. Phosphoric acid, dimethyl sulfoxide, and *N*,*N*-dimethylformamide were purchased from Junsei. Dimethyl sulfoxide-d_6 (DMSO-d_6) used in NMR experiments were Sigma–Aldrich products.

2.2. Synthesis of the precursor polymer

The precursor polymer, poly-(succinimide) (PSI), was synthesized via acid-catalyzed polycondensation of L-aspartic acid using phosphoric acid as the catalyst [29–31]. Purified PSI (0.97 g, 10 mmol succinimide unit) was dissolved in water-free DMF (7 mL), followed by aminolysis with 10 mol% of octadecylamine at 70 °C for 25 h. (PSI-*g*-C_{18}). The reaction mixture was precipitated twice in cold ether and dried in vacuo at 50 °C.

2.3. Synthesis of as-synthesized iron oxide nanoparticles

As-synthesized iron oxide nanoparticles were produced by a seed-mediated growth method using 6 nm nanoparticles synthesized using a thermal decomposition method [8] Briefly, to synthesize nanoparticles 6 nm in diameter, iron (III) acetylacetonate (2 mmol), 1,2-hexadecanediol (10 mmol), oleic acid (6 mmol), oleyl-amine (6 mmol), and benzyl ether (20 mL) were mixed in a three-neck round flask under an N_2 atmosphere. Next, the mixture was heated to 200 °C for 2 h and further heated to 300 °C for 1 h under reflux. After the mixture was cooled to room temperature, excess ethanol was used to wash the reactant. Nanoparticles were collected by centrifugation.

2.4. Preparation of poly(amino acid)-coated iron oxide nanoparticles (PAION)

First, 18 mg of PSI graft copolymer (PSI-*g*-C_{18}) and 18 mg iron oxide nanoparticles were dissolved in 2.2 mL of a mixed solvent (THF [tetrahydrofuran]: DMF [*N*,*N*-dimethylformamide] = 4:1,v/v). (the molar ratio between the amounts of PSI-g-C_{18} and nanoparticles was over 300). The solution was constantly stirred for 0.5 h, and the mixture was subsequently added dropwise to 18 mL of aqueous solution of NaOH, NH_4OH, 2-aminoethanol, or *N*,*N*-dimethylethylene-diamine to synthesize the PAsp-, PAsn, PHEA-, or PDMAEA-coated iron oxide nanoparticles, respectively. After 24 h of stirring, the mixture was dialyzed against DDI water to remove mixed organic solvent (THF and DMF), and centrifuged (6000 rpm, 10 min) to remove the uncoated nanoparticles. Finally, PAIONs were selectively collected by centrifugation at 15,000 rpm for 1 h.

2.5. Characterization of poly(amino acid)s coated iron oxide nanoparticles (PAIONs)

Transmission electron microscopy (TEM) was obtained using a Philips CM-200 instrument operating at 200 kV. A solution of poly(amino acid)-coated iron oxide nanoparticles containing 0.1% (w/v) phosphotungstic acid (PTA; a negative stain) was placed on a copper grid covered with a formvar carbon membrane. The grid was exposed to air enough to evaporate the solvent. Nanoparticle sizes were measured by dynamic light scattering instrument (ELS-Z2, particle size analyzer & Zeta potential, Otsuka electronics Co., Ltd., Japan). Fourier transform infrared (FTIR) spectra were recorded using a Spectrum GX & AutoImage instrument (Perkin–Elmer) at room temperature. Spectra were recorded in the range 4000–450 cm^{-1} using KBr pellets. The TGA was carried out on a setsys 16/18 (Setaram, France). We analyzed the iron oxide nanoparticles and PAIONs at a temperature range of 30–1000 °C. The saturation of magnetization was evaluated using a vibrating-sample magnetometer (Lakeshore, model 955287(A)). The atomic weight percentage of Fe in each PAION was measured by inductively-coupled plasma atomic emission spectrometer (ICP-AES, model: Jarrell Ash IRIS-AP, Thermo) for further in vitro study.

2.6. MRI phantom study

All MR imaging experiments were performed using a 4.7 T clinical MRI instrument (Bruker BioSpec 47/40). The parameters were as follows for T_2 relaxivity coefficients: TE = 7.4 ms, TR = 8,000 ms, FOV = 5.5 cm × 5.5 cm, matrix = 128 × 128, slice thickness = 2 mm.

2.7. Cell culture and cytotoxicity test

MDA-MB 231 and KB cell lines were provided from professor Dai-Wu Seol (BioNano Research Institute, Kyungwon University, Korea), and the Korean cell bank, respectively. These cell lines were cultured in Dulbecco's modified Eagle medium (DMEM) with Glutamax-1 supplemented with 10% FBS (Gibco-BRL) and 1% antibiotics/antimycotics (100 units/mL penicillin and streptomycin) and maintained at 37 °C in a humidified atmosphere of 5% CO_2. The cells were passaged at sub-confluence and plated on culture petri dish.

The cells were plated at a concentration of 5×10^4/mL for 24 h prior to the experiment. To test cytotoxicity of the nanoparticles, 10 μL of nanoparticle solution of a predetermined concentration was added into each well and incubated for 24 h, and 48 h. After the indicated time, the 10 μL of MTT solution of 5 mg/mL was also added followed by incubation for 4 h. The formed formazan crystal was dissolved in 100 μL of lysis buffer (DMF 50 v/v%, SDS 20 w/v%, acetic acid, pH 4.7). The absorbance of the sample proportional to the cell viability was measured at 570 nm with a background absorbance at 650 nm.

2.8. Prussian blue staining

2.5×10^4 cells of MDA-MB 231 and KB cell lines were seeded on each well of 8-chamber slide and grown for 24 h. Then the cells

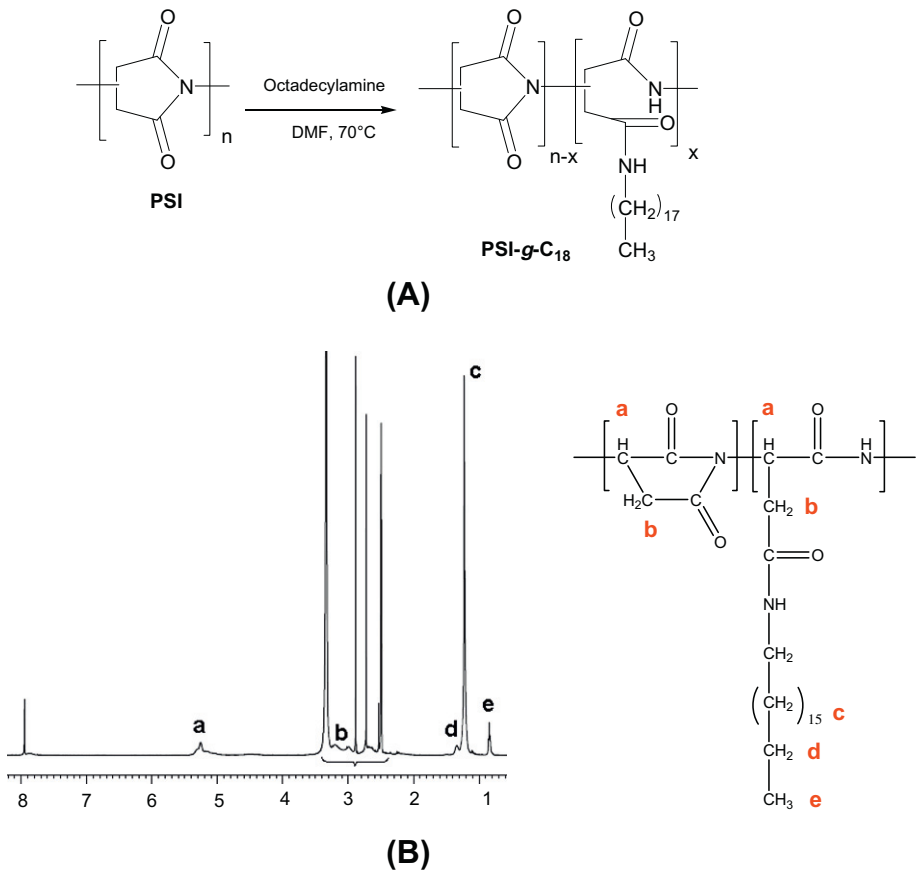

Fig. 1. (A) synthetic route of octadecyl grafted poly(succinimide)(PSI-*g*-C_{18}),precursor polymer and (B) ^{1}H NMR spectra of PSI-*g*-C_{18} in DMSO-d_6.

were incubated with a PAION containing medium. After 12 or 24 h, the medium was removed and the cells were washed with PBS solution. The cells were stained according to the manufacturer's protocol (Prussian Blue Iron Stain Kit, Polyscience, PA, USA). Briefly, the PAION-labeled and control cells were incubated with 1:1 mixture of 4% potassium ferrocyanide and 4% hydrochloric acid for 20 min, and washed with distilled water several times. To stain the nuclei of the cells, a Nuclear Fast Red solution (Polyscience, PA, USA) treated the cells for 5 min and then rinsed in running tap water for 1 min. The cells were then observed using light microscopy (Carl Zeiss Microscopy, Gottingen, Germany).

3. Results and discussion

3.1. Synthesis of PSI-g-C_{18} and iron oxide nanoparticles

A precursor polymer was synthesized according to the synthetic route as shown in Fig. 1A. Octadecylamine was successfully conjugated to PSI by aminolysis in DMF. The chemical structure of octadecyl grafted PSI (PSI-*g*-C_{18}) was confirmed by Fourier transform infrared (FT-IR) analysis and ^{1}H NMR spectroscopy (Fig. 1B). The peak at 5.3 ppm was assigned to the methane protons of the succinimide unit, respectively, while peaks at 0.8, 1.2 and 1.3 ppm (marked with symbols) were assigned to the octadecyl chain [29–33]. The grafted mole percentage, defined as the degree of substitution (DS), of C_{18}, was 12.43. The FT-IR spectrum of PSI-*g*-C_{18} (see Fig. S1) shows the characteristic adsorption bands of succinimide at 1711 cm^{-1}. The C—H stretch of the grafted octadecyl chain exhibits absorption bands at 2800–3000 cm^{-1}. The two peaks that appeared at 1648 and 1532 cm^{-1} are ascribed to C=O stretching and N—H bending of the amide groups in PSI-*g*-C_{18}. PSI was aminolyzed with 2-aminoethanol for conversion into PHEA to determine the molecular weight (Mn) of PHEA by a gel permeation chromatography (GPC). The obtained molecular weight (M_n) of PHEA was 19 800 Da (polydispersity index = 1.32) [31].

Monodispersed iron oxide nanoparticles were synthesized by a thermal decomposition method [8]. The as-synthesized nanoparticle morphology was confirmed via TEM analysis and the average diameters of the nanoparticles obtained from size histograms was 13.27 ± 1.67 nm (see Fig. S2). The crystal and chemical structure of the nanoparticles were confirmed by using X-ray diffraction (XRD) and Fourier transform infrared (FT-IR) (see Fig. S3). In Fig. S3a, all peaks matched well with values previously reported for magnetite (Fe_3O_4) crystals. These Fe_3O_4 nanoparticles are not soluble in water due to the presence of the hydrophobic ligand, oleate/oleylamine. For bio-application, it is essential to transfer nanoparticles from the organic phase to an aqueous phase.

3.2. Poly(amino acid) coated iron oxide nanaoparticles

As shown in Scheme 1, PSI-*g*-C_{18} was introduced as a precursor polymer to coat the hydrophobic nanoparticles and prepare water-dispersible, stable magnetic nanoparticles. However, PSI-*g*-C_{18} cannot be directly used to stabilize hydrophobic nanoparticles in water because the PSI backbones are also not soluble in water [29–32]. PSI can be easily aminolyzed with nucleophilic compounds to form various poly(amino acid)s known to be biodegradable, biocompatible, and water-soluble (Scheme 2). Aqueous solutions of NaOH [31], NH_4OH [32], 2-aminoethanol [33], and *N*,*N*-dimethylethylene-diamine [41] were selected to synthesize

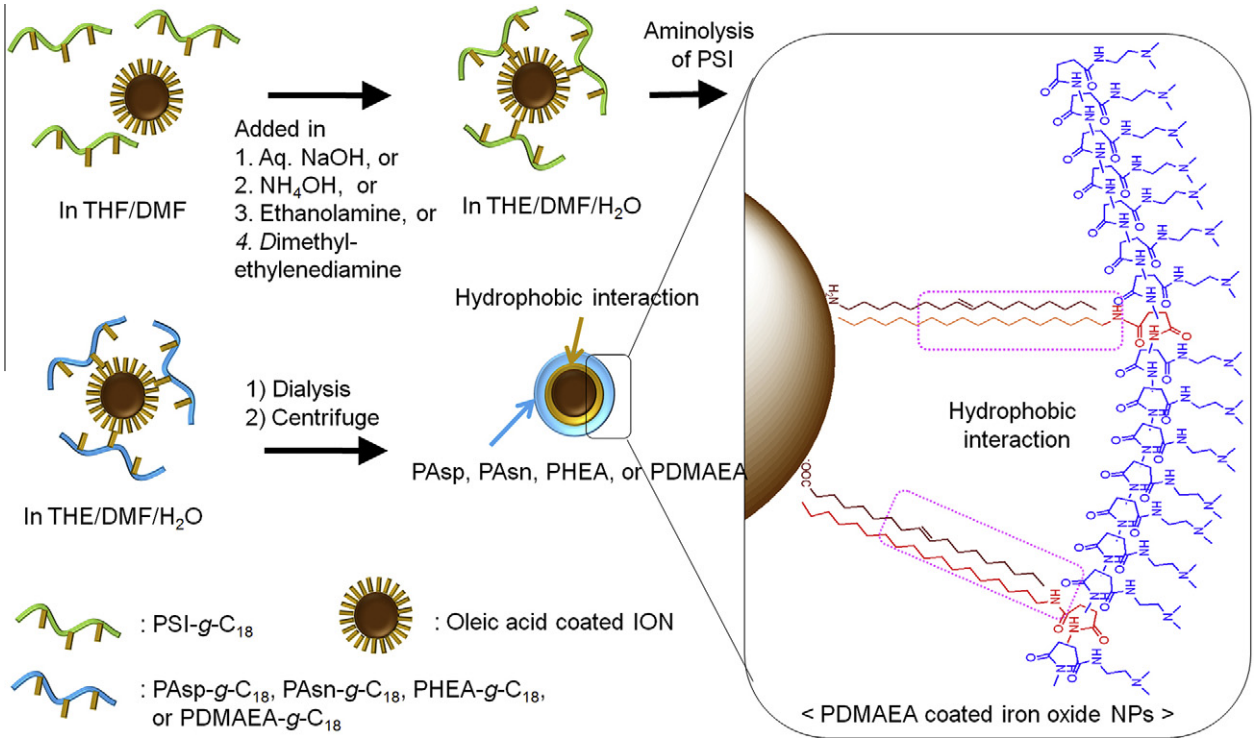

Scheme 1. Schematic diagram of novel method to synthesize a poly(aspartic acid) (PAsp), poly(asparagines) (PAsn), poly(2-hydroxy-ethyl L-aspartamide) (PHEA), and poly-α,β-(N-2-dimethylaminoethyl L-aspartamide) (PDMAEA) coated iron oxide nanoparticles.

the poly(aspartic acid) (PAsp), poly(asparagines) (PAsn), poly (2-hydroxy-ethyl L-aspartamide) (PHEA), and poly-α,β-(*N*-2-dimethylaminoethyl L-aspartamide) (PDMAEA) backbone from PSI-*g*-C_{18}, respectively. The THF/DMF mixture solution containing the hydrophobic nanoparticles and precursor polymer, PSI-g-C_{18}, were added to the water solution. Upon vortexing, the amphiphilic graft copolymer containing a hydrophilic poly(amino acid) backbone and hydrophobic alkyl side chain(C_{18}) was synthesized by aminolysis of the succinimide unit in the PSI-*g*-C_{18}. Hence, the hydrophobic nanoparticles were coated with various poly(amino acid) via hydrophobic interactions between the octadecyl chain of amphiphilic graft copolymer and the oleate/oleylamine alkyl tails on the nanoparticles. Thus, the hydrophilic poly(amino acid) backbone rendered the hydrophobic nanoparticles dispersed aqueous solutions.

Fig. 2 shows the phase transfer of the hydrophobic nanoparticles from an organic to an aqueous phase after coating. Poly(amino acid) coated iron oxide nanoparticles, PAIONs, in water, did not proceed to an hexane phase, indicating that hydrophobilic PAsp, PAsn, PHEA, PDMAEA were successfully synthesized and exposed to the surrounding aqueous environment. Fig. 3 shows the transmission electron microscopy (TEM) images of the PAIONs in aqueous solution; the PAIONs were negatively stained with phosphotungstic acid (2 wt.%). The TEM images (Fig. 3a–d) showed that the nanoparticles were successfully coated with "bright" unstained PAsp, PAsn, PHEA, PDMAEA polymers, repectively. The average diameters of various poly(amino acid) coated iron oxide nanoparticels were about less than 20 nm. The poly(amino acid) coated iron oxide nanoparticles were covered by polymer shell with a uniform thicknesses. The number-weighted size distribution of the PAsp, PAsn, PHEA, PDMAEA coated iron oxide nanoparticles determined using dynamic light scattering were 33.1 ± 8.3 nm, 25.8 ± 6.4 nm, 24.8 ± 6.3 nm, 24.5 ± 6.1 nm in aqueous solution, respectively (Fig. 4, please see Fig. S4 for intensity-weighted size distribution). The size of the PAsp coated iron oxide nanoparticles was slightly greater than other PAIONs. This suggests that several iron oxide nanoparticles encapsulated in the same polymer shell were also formed. The surface charges of PAIONs were characterized with zeta-potential measurement (Table 1). The zeta potential for the PAsp-coated, PAsn-coated, PHEA-coated, and PDMAEA-coated iron oxide nanoparticles were −49.83 mV, −34.23 mV, −10.39 mV, and +6.21 mV, respectively. Therefore, each poly(amino acid) was located at the outermost surface, and was swollen in the water with specific charges. Zeta-potentials of four PAIONs confirm the surface functional group and the repulsive stabilization of the nanoparticles. All PAIONs are also stable in various pH conditions between pH4 and 10, and the PAION size did not change in PBS buffer solution for at least 4 days (Fig. 5). These results indicated that PAIONs have excellent colloidal stability in physiological conditions required for in vivo applications.

Fourier transform infrared (FTIR) analysis was used to confirm the attachment of each poly(amino acid)s on the iron oxide nanoparticles surface. Compared with FT-IR spectrum of PSI-*g*-C_{18} (Fig. S1), Fig. 6a–d shows the characteristic peaks of poly(amino acid) at 3379–3420 cm^{-1} (NH), 1652 cm^{-1} (amide I), and 1540 cm^{-1} (amide II), while, the characteristic peak of PSI at 1711 cm^{-1} disappeared completely, suggesting that all the succinimide units were convert into the amide unite [42]. In addition, Fe—O vibration bands were observed at 591–599 cm^{-1}. These results suggested that the hydrophobically stabilized iron oxide nanoparticles were easily and successfully coated with various poly(amino acid) by simply controlling the reaction solution during the surface coating.

The iron oxide nanoparticle contents of the as-synthesized nanoparticles and PAIONs were determined by thermal gravimetric analysis (TGA) (see Fig. S5). The weight percentages of iron oxide for oleic acid and poly(amino acid) coated nanoparticles were 87.2%, 64.7%, 61.1%, 60.7%, and 57.2% in order of oleate/

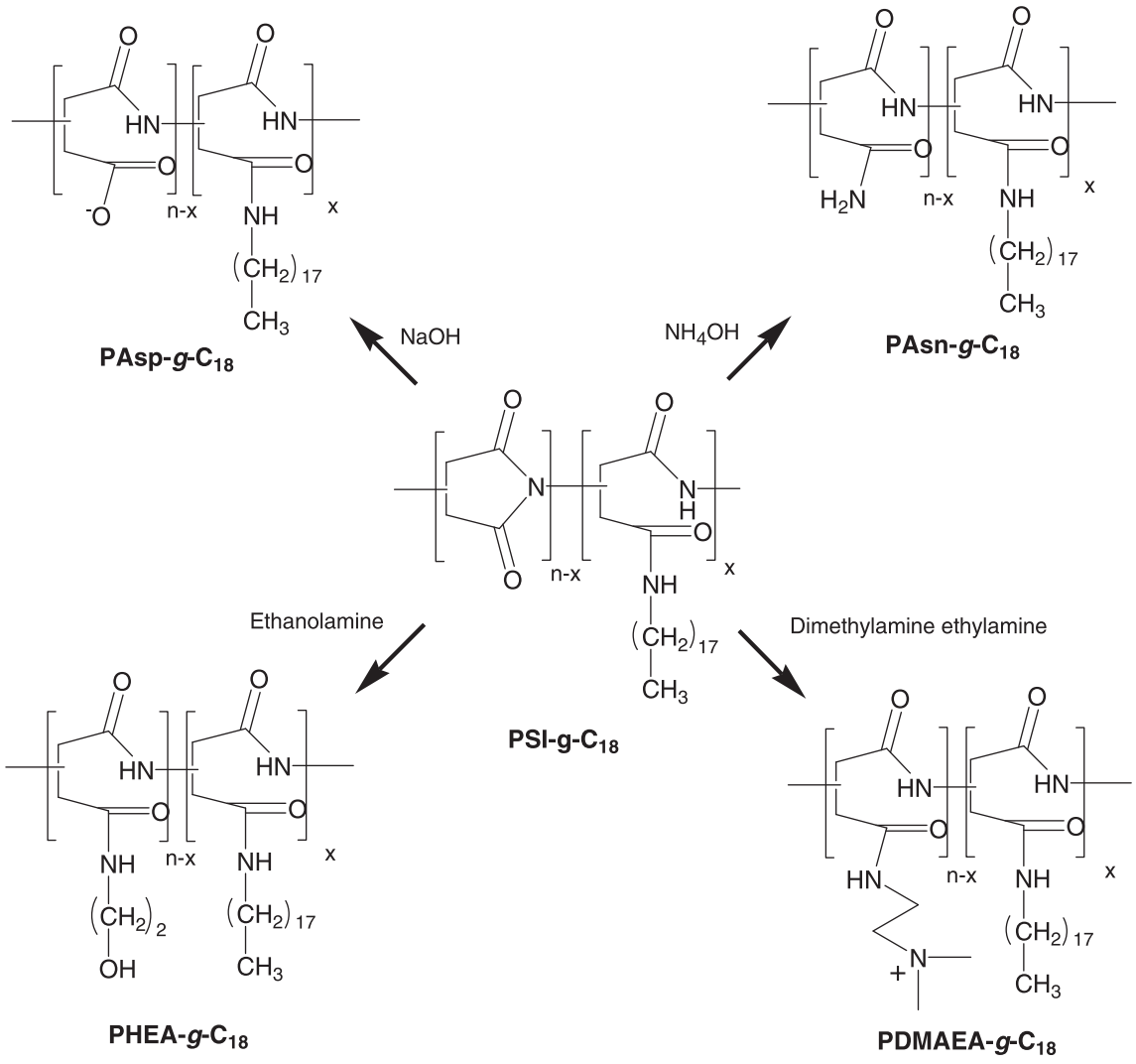

Scheme 2. Synthetic route of various poly(amino acid)s by aminolysis of poly(succinimide) with NaOH, NH_4OH, 2-aminoethanol, and *N*,*N*-dimethylethylene-diamine in aqueous solution.

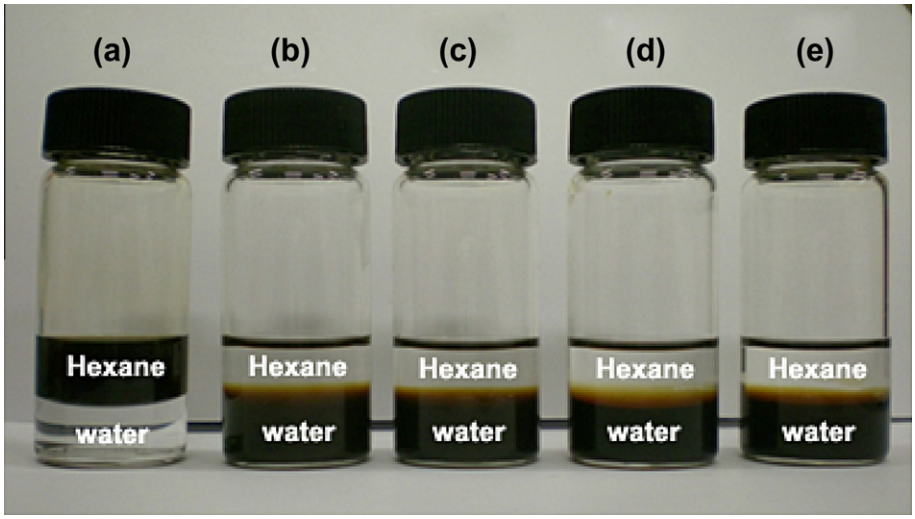

Fig. 2. (a) hexane solution of as-synthesized iron oxide nanopartilces and water solution of (b) PAsp-, (c) PAsn-, (d) PHEA-, (e) PDMAEA-coated iron oxide nanoparticles.

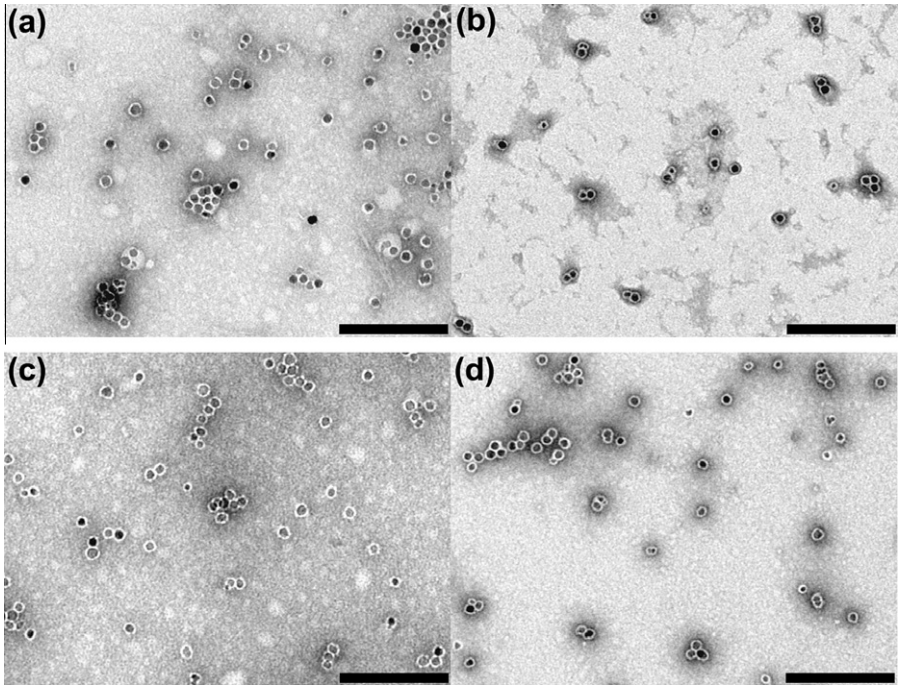

Fig. 3. TEM images of: (a) PAsp-, (b) PAsn-, (c) PHEA-, and (d) PDMAEA-coated iron oxide nanoparticles in water. All scale bars: 200 nm.

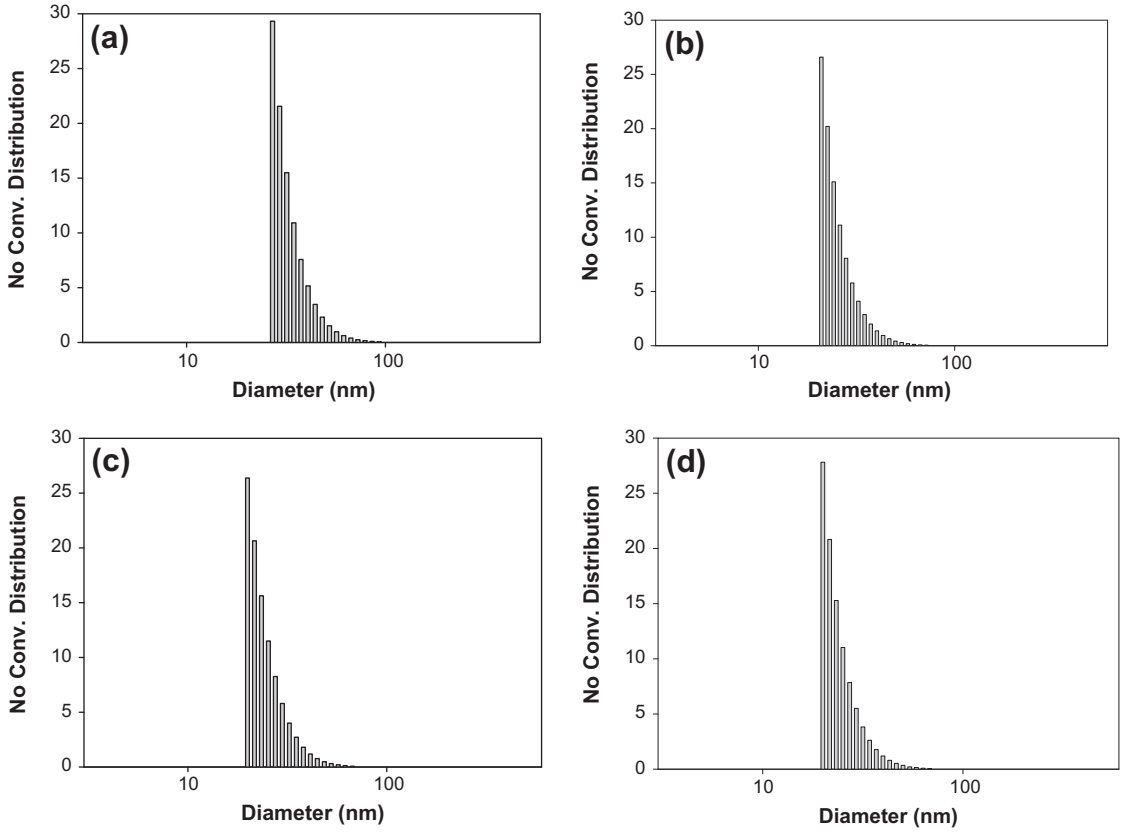

Fig. 4. Size distribution of: (a) PAsp-, (b) PAsn-, (c) PHEA-, and (d) PDMAEA-coated iron oxide nanoparticles determined using DLS in water.

oleylamine-, PAsp-, PAsn-, PHEA-, PDMAEA-coated iron oxide nanoparticles, respectively. The encapsulation efficiency is defined as the obtained amount of Fe_3O_4 nanoparticles divided by the used amount of Fe_3O_4 nanoparticles per 100 mg of PAION. The encapsulation efficiency of PAION was 61.01%.

3.3. Magnetic properties of PAIONs

The magnetic sensitivity of the as-synthesized nanoparticles and PAIONs were examined by a vibrating sample magnetometer at 300 K (Fig. 7). The as-synthesized nanoparticles and PAIONs

Table 1
Characterization results of PAsp-, PAsn-, PHEA-, and PDMAEA-coated iron oxide nanoparticles.

	1	2	3	4
Shell component	PAsp	PAsn	PHEA	PDMAEA
Surface charge	−49.83 ± 0.23	−34.23 ± 0.23	−10.39	+6.21 ± 2.43
Diameter (DLS, nm)[a]	33.1 ± 8.3	25.8 ± 6.4	24.8 ± 6.3	24.5 ± 6.1
Iron oxide content[b]	64.7%	61.1%	60.7%	57.2%
M_s[c] (emu g^{-1} PAION)	46.9	40.5	40.0	36.8
r_2[d] (L $mmol^{-1}$ s^{-1})	265	253	250	247

[a] Average diameter measured by DLS.
[b] Iron oxide nanoparticles content measured by TGA.
[c] M_s = saturation magnetization. (emu g^{-1} PAION).
[d] $r_2 = T_2$ relaxivities coefficient at 4.7 T.

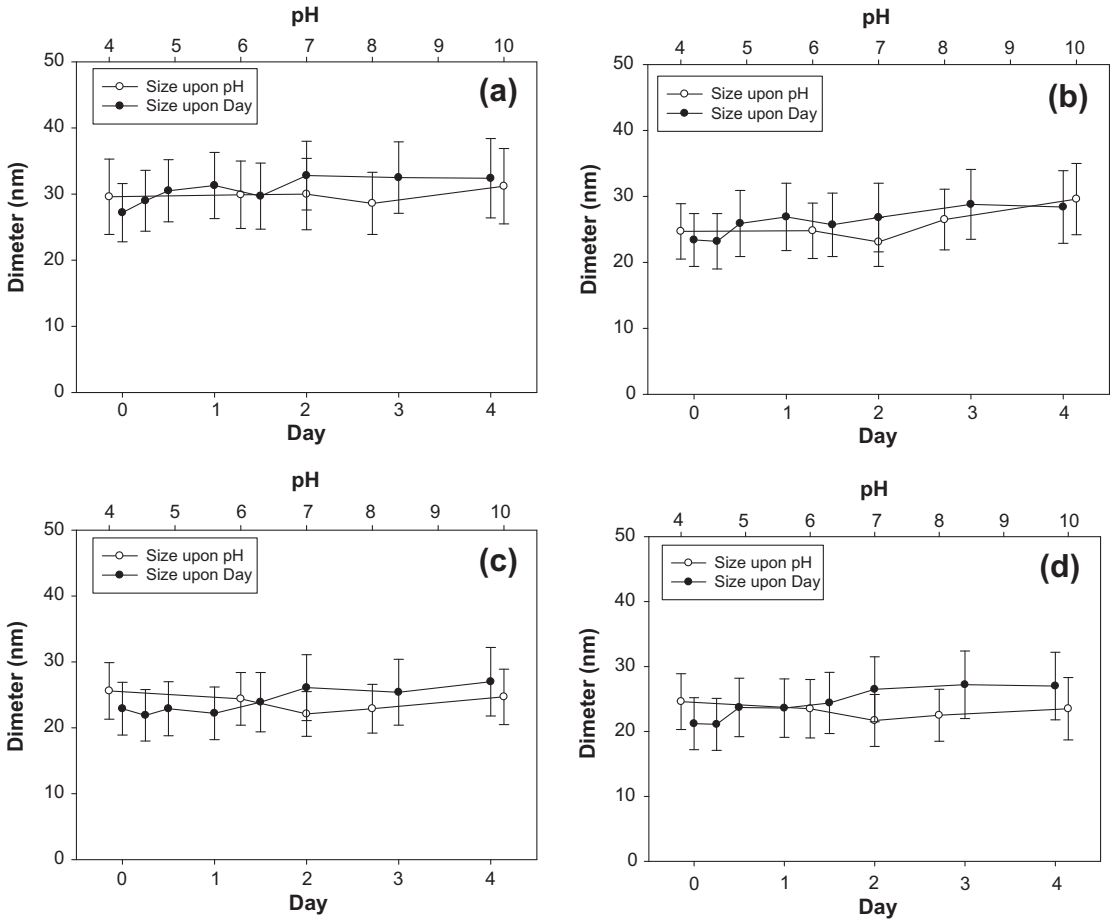

Fig. 5. Stability test of each poly(amino acid) coated iron oxide nanoaprticles by measuring of the size distribution with time and pH variance.

exhibited superparamagnetic behaviors. The saturation magnetizations (M_s values) at 1.5 T of the as-synthesized nanoparticles and PAIONs were 73.0 emu g^{-1} Fe_3O_4, 46.9 emu g^{-1}, 40.5 emu g^{-1}, 40.0 emu g^{-1}, and 36.8 emu g^{-1} PAION, respectively. Because of the presence of poly(amino acid)s, the saturation of magnetization of PAIONs were lower than that of Fe_3O_4 nanoparticles. Based on the TGA results, the normalized M_s value of PAsp-coated nanoparticles (72.5 emu g^{-1} Fe_3O_4) was equivalent to that of the original iron oxide nanoparticles, indicating that the surface coating process did not change the nanoparticle magnetic properties. However, the normalized M_s values of PAsn-, PHEA-, PDMAEA-coated iron oxide nanoparticles (about 66 emu g^{-1} Fe_3O_4) were a little lower than that of original nanoparticles.

The relaxation times T_2 of the PAIONs in water at various concentrations were measured at 4.7 T to evaluate the utility of the PAIONs as MRI contrast agents. As the concentration of the PAIONs increased, the signal intensity of the spin–spin relaxation time (T_2)-weighted MRI image decreased (Fig. 8A). This behavior indicates that each PAION may be used as T_2 MRI contrast agents. The T_2 relaxivity coefficients (r_2 values) were measured by the change in the spin–spin relaxation rate (T_2^{-1}) per unit Fe concentration. The r_2 values were calculated to be 265, 253, 250, and 247 L $mmol^{-1}$ s^{-1} for PAsp-, PAsn-, PHEA-, PDMAEA-coated iron oxide nanoparticles, respectively (Fig. 8B). The r_2 value of PAsp-coated iron oxide nanoparticles was slightly higher than other PAIONs due to the aggregation effect of several iron oxide

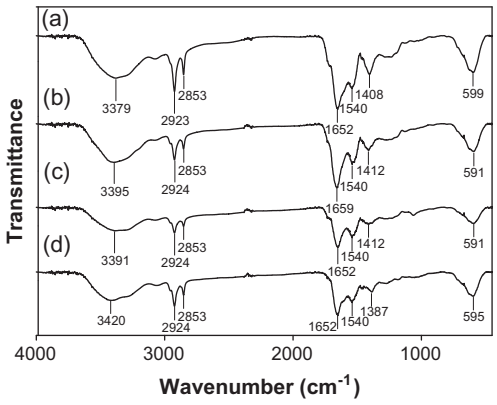

Fig. 6. FTIR spectra of: (a) octadecyl grafted poly(succinimide)(PSI-*g*-C_{18}), (b) PAsp-, (c) PAsn-, (d) PHEA-, and (e) PDMAEA-coated iron oxide nanoparticles ν_s = symmetric stretching vibration; ν_{as}: asymmetric stretching vibration; δ = bending vibration.

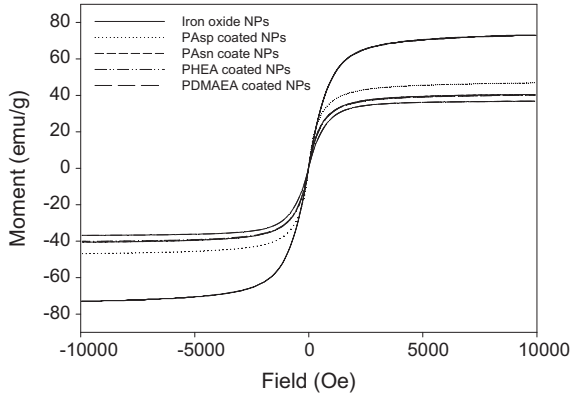

Fig. 7. Magnetic hysteresis loops of as-synthesized iron oxide nanoparticles and each poly(amino acid) coated iron oxide nanoparticles (PAION) determined by VSM at room temperature, respectively.

nanoparticles encapsulated in the PAsp shell [20]. Ferridex and resovist are well-known commercial MRI contrast agents. The r_2 values of ferridex and resovist (at 4.7 T), were 105 L mmol^{-1} s^{-1} and 176 L mmol^{-1} s^{-1}, respectively [43]. It can be seen that r_2 values of the PAIONs were higher than those of ferridex and resovist at 4.7 T.

3.4. Cell viability and cellular uptake of PAIONs

An MTT assay using the KB and MDA-MB231 cell lines was performed to analyze the biocompatibility of the PAIONs. The PAIONs at five different concentrations, ranging from 0.0625 mg mL^{-1} to 0.5 mg mL^{-1} were incubated with KB and MDA-MB231 cell lines for 24 h and 48 h. (Fig. 9). Both cell lines retained high cell viability in the MTT assay even at high concentrations. The results indicate that the PAIONs are reasonably non-toxic and biocompatible. Many groups reported that nano-sized iron oxide nanoparticles can be biodegraded in lysosomes of monocyte phagocytes system cells [44,45], and Kupffer cells in liver can degrade them and can incorporate most of the iron into ferritin [45,46]. PAIONs can be also biodegradable because poly(amino acid) shell are entirely degraded by proteolytic enzymes in the body.

The KB cell lines were treated with each PAIONs to evaluate the cellular internalization. Prussian blue staining of the KB cell lines treated with the PAIONs was performed for 24 h (Fig. 10). The cellular uptake of the PAIONs was highly dependent on the type of surface charge. Negatively charged PAsp-, PAsn, and PHEA-coated iron oxide nanoparticles were not observed inside cells. No Prussian blue staining was observed for cells at 0.1 mg Fe/mL of PAsp-, PAsn, and PHEA-coated iron oxide nanoparticles, indicating that these PAIONs were not internalized into cells. However, PDMAEA coated iron oxide nanoparticles were detected inside the cells, which is attributed to the cellular binding of positively charged nanoparticles to negatively charged cells. These results are in good agreement with the previous reported results, where positively charged nanocarriers could be more easily delivered into cells than negatively charged and neutral charged nanocarriers [12–14]. Therefore, we conclude that PAIONs that are positively charged are efficiently internalized into KB cells.

From the Prussian blue staining and MRI results, PDMAEA coated iron oxide nanoparticles is evaluated to be excellent MRI contrast agent on the basis of their high MR contrast capability and efficient intracellular delivery. Furthermore, they would easily accumulate in tumors through the enhanced permeability and retention (EPR) due to the long mean blood circulation time attributable to their small hydrodynamic size less than 40 nm [2,7].

Although PAsp-, PAsn, and PHEA-coated iron oxide nanoparticles were not internalized into KB cells well, those nanoparticles can be also applied as cancer targeting T_2 contrast agent after coupling with cancer targeting agents that will specifically recognize cancer markers such as Her2/neu and a folate receptor. We recently reported the Her2/neu antibody conjugated PHEA coated

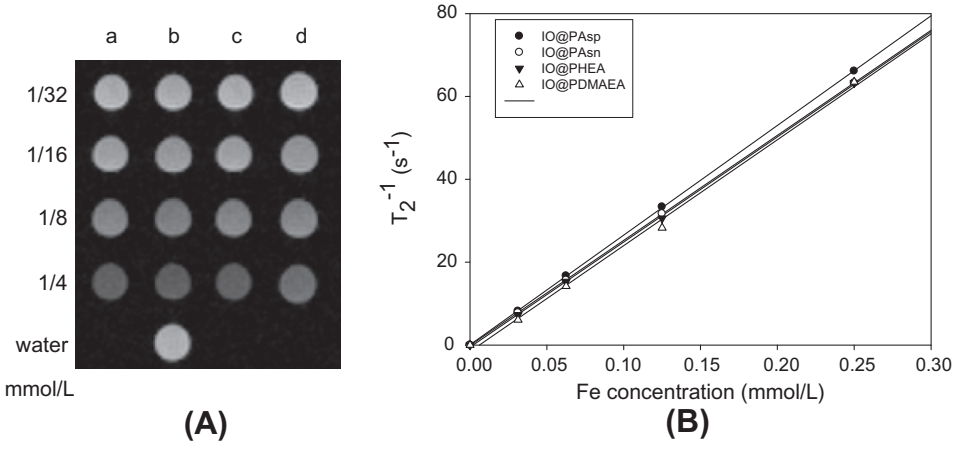

Fig. 8. (A) T_2-weighted MR images of each PAION in aqueous solution with various concentrations at 4.7 T: (a) PAsp-, (b) PAsn-, (c) PHEA-, and (d) PDMAEA-coated iron oxide nanoparticles, and (B) Graphs of R_2 against the iron concentration of each PAION.

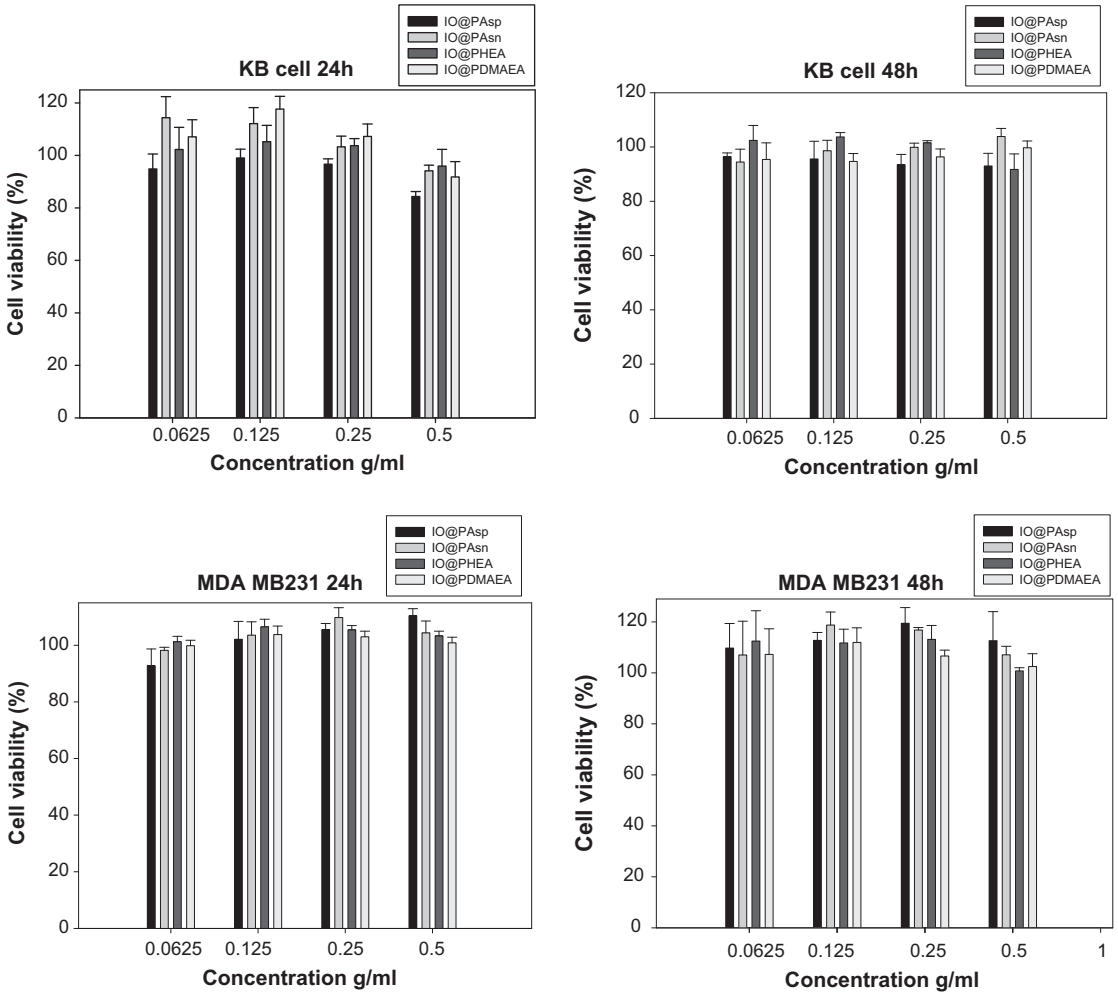

Fig. 9. Cell viability of KB cells treated with various concentrations of each PAION measured by the MTT assay for 24 h and 48 h.

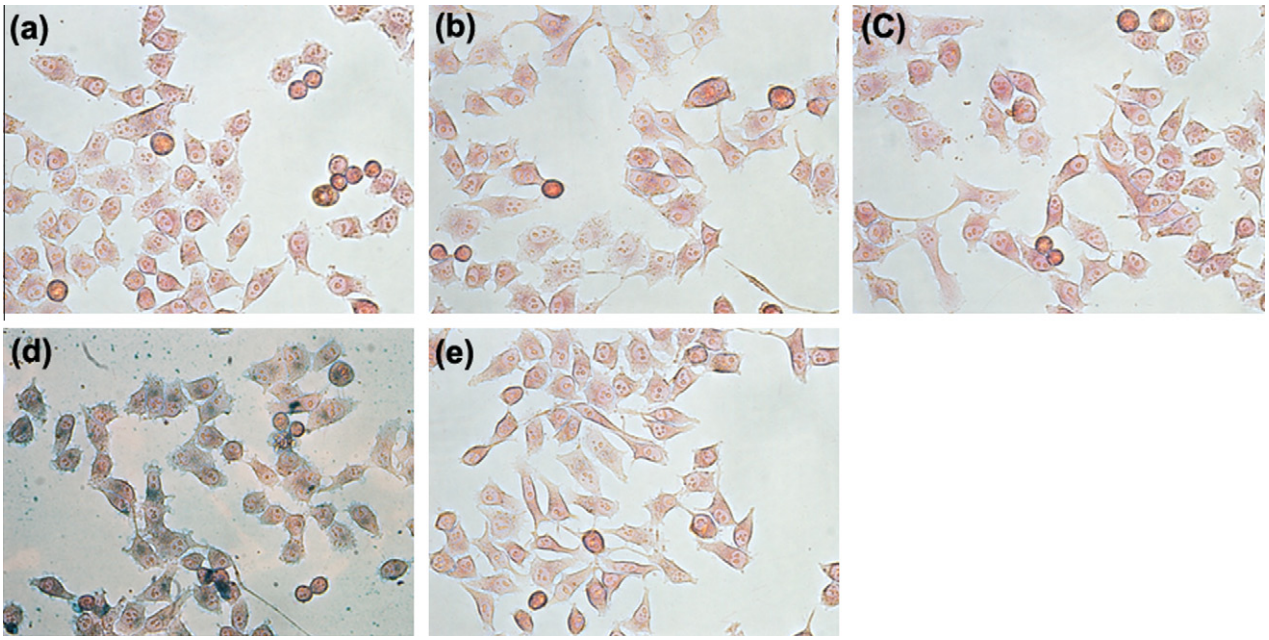

Fig. 10. Prussian blue staining images of KB cells treated with 0.1 mg Fe/mL of: (a) PAsp-, (b) PAsn-, (c) PHEA-, and (d) PDMAEA-coated iron oxide nanoparticles, and (e) control for 24 h.

iron oxide nanoparticles which showed specific breast cancer targeting ability [40]. PAsp- and PAsn-coated iron oxide nanoparticles could be also easily conjugated with cancer targeting moiety because both of them have functional groups on the surface of nanoparticles such as carboxylic groups for PAsp. According to our successful results, various PAIONs prepared using one precursor polymer via simple coating method have good potential as new T_2 weighted MRI contrast agents.

4. Conclusion

This report demonstrates that simple coating procedure by using the poly(succinimide) as a precursor polymer to coat the iron oxide nanoparticles with various poly(amino acid) derivatives. The hydrophobic interaction between iron oxide nanoparticles and hydrophobic alkyl chain grafted on poly(amino acid) backbone stabilize the PAION in aqueous solution. The diameters of the PAIONs are in the range of 20–29 nm and are maintained in aqueous solutions with a wide range of pH and at least 4 days. Further, all PAIONs show high T_2 relaxivity coefficients (r_2 values) and no cytotoxicity. Prussian blue staining of cells treated with PAIONs indicates a strong uptake for positively charged PAIONs due to the ionic interaction with negatively charged cell membranes. Therefore, PAIONs can be used for various biomedical applications such as, diagnosis of cancer, and cell labeling.

Acknowledgments

This work was supported by the R&D Program through the NRF funded by the Ministry of Education, Science and Technology of the Korean government. We would like to thank staffs of KBSI for their assistance with the TEM measurements and Ochang KBSI for their assistance with MRI measurements.

Appendix A. Supplementary material

Supplementary data associated with this article can be found, in the online version, at http://dx.doi.org/10.1016/j.jcis.2012.09.044.

References

[1] S.-J. Lee, J.-R. Jeong, S.-C. Shin, J.-C. Kim, Y.-H. Chang, Y.-M. Chang, J.-D. Kim, J. Magn. Magn. Mater. 272 (276) (2004) 2432.
[2] A. Ito, Y. Kuga, H. Honda, H. Kikkawa, A. Horiuchi, Y. Watanabe, T. Kobayashi, Cancer Lett. 212 (2004) 167.
[3] N. Kohler, C. Sun, J. Wang, M. Zhang, Langmuir 21 (2005) 8858.
[4] R. Qiao, C. Yang, M. Gao, J. Mater. Chem. 19 (2009) 6274.
[5] J. Lee, Y.-M. Huh, Y. Jun, J. Seo, J. Jang, H. Song, S. Kim, E. Cho, H. Yoon, J. Suh, J. Cheon, Nat. Med. 13 (2007) 95.
[6] Y.-M. Huh, J. Am. Chem. Soc. 127 (2005) 12387.
[7] Y.-w. Jun, J.-H. Lee, J. Cheon, Angew. Chem. Int. Ed. 47 (2008) 5122.
[8] S.H. Sun, H. Zeng, D.B. Robinson, S. Raoux, P.M. Rice, S.X. Wang, G.X. Li, J. Am. Chem. Soc. 126 (2004) 273.
[9] W. Xingyong, L. Hongjian, L. Jianquan, N.H. Kari, A.T. Joseph, L.J. Peter, G. Nianfeng, P. Frank, P.B. Marcel, Nat. Biotechnol. 21 (2003) 41.
[10] P. Teresa, M. Liberato, K. Stefan, L. Tim, K. Dmitry, L.R. Andrey, K. Simon, R. Joachim, N. Giovanni, J.P. Wolfgang, Nano Lett. 4 (4) (2004) 703.
[11] A. Verma, F. Stellacci, Small 6 (1) (2009) 12.
[12] A.K. Gupta, M. Gupta, Biomaterials 26 (2005) 3995.
[13] Y. Lee, K. Miyata, M. Oba, T. Ishii, S. Fukushima, M. Han, H. Koyama, N. Nishiyama, K. Kataoka, Angew. Chen. Int. Ed. 47 (2008) 5163.
[14] E.C. Cho, J.W. Xie, P.A. Wurm, Y.N. Xia, Nano Lett. 9 (2009) 1080.
[15] H.B. Na, I.S. Lee, H. Seo, Y.I. Park, J.H. Lee, S.-W. Kim, T. Hyeon, Chem. Commun. 48 (2007) 5167.
[16] C.-A.J. Lin, R.A. Sperling, J.K. Li, T.-Y. Yang, P.-Y. Li, M. Zanella, W.H. Chang, W.J. Parak, Small 4 (3) (2008) 334.
[17] E. Amstad, T. Gillich, I. Bilecka, M. Textor, E. Reimhult, Nano Lett. 9 (12) (2009) 4042.
[18] J. Xie, C. Xu, N. Kohler, Y. Hou, S. Sun, Adv. Mater. 19 (2007) 3163.
[19] J. Qin, S. Laurent, Y.S. Jo, A. Roch, M. Mikhaylova, Z.M. Bhujwalla, R.N. Muller, M. Muhammed, Adv. Mater. 19 (2007) 1874.
[20] H. Ai, C. Flask, B. Weinberg, X.-T. Shuai, M.D. Pagel, D. Farrell, J. Duerk, J. Gao, Adv. Mater. 17 (16) (2005) 1949.
[21] C. Fang, N. Bhattarai, C. Sun, M. Zhang, Small 5 (14) (2009) 1637.
[22] H.-M. Yang, C.W. Park, S. Lim, S.-I. Park, B.H. Chung, J.-D. Kim, Chem. Commun. 47 (2011) 12518.
[23] C. Barrera, A.P. Herrera, C. Rinaldi, J. Colloid Interface Sci. 329 (2009) 107.
[24] H. Basti, L.B. Tahar, L.S. Smiri, F. Herbst, M.-J. Vaulay, F. Chau, S. Ammara, S. Benderbous, J. Colloid Interface Sci. (2010) 248.
[25] H.-M. Yang, H.J. Lee, C.W. Park, S.R. Yoon, S. Lim, B.H. Chung, J.-D. Kim, Chem. Commun. 47 (2011) 5322.
[26] J. Szebeni, Toxicology 216 (2005) 106.
[27] T. Ishida, R. Maeda, M. Ichihara, K. Irimura, H. Kiwada, J. Controlled Release 88 (2003) 35.
[28] K. Knop, R. Hoogenboom, D. Fischer, U.S. Schubert, Angew. Chen. Int. Ed. 49 (36) (2010) 6288.
[29] S.R. Yang, S.B. Kim, C.O. Joe, J.-D. Kim, J. Biomed. Mater. Res. A 86 (2008) 137.
[30] H.S. Kang, J.-D. Kim, S.-H. Han, I.-S. Chang, J. Controlled Release 81 (2002) 135.
[31] H.S. Kang, S.R. Yang, J.-D. Kim, S.-H. Han, I.-S. Chang, Langmuir 17 (2001) 7501.
[32] H.J. Lee, S.R. Yang, E.J. An, J.-D. Kim, Macromolecules 39 (2006) 4938.
[33] S.R. Yang, H.J. Lee, J.-D. Kim, J. Controlled Release 114 (2006) 60.
[34] J.H. Jeong, H.S. Kang, S.R. Yang, J.-D. Kim, Polymer 44 (2003) 583.
[35] J.M. Anderson, D.F. Gibbons, R.L. Martin, A. Hiltner, R. Woods, J. Biomed. Mater. Res. A 5 (1974) 197.
[36] J. Drobnik, Adv. Drug Deliv. Rev. 3 (1989) 229–245.
[37] R. Mendichi, G. Giammona, G. Cavallaro, G. Schieroni, Polymer 41 (2000) 8649.
[38] B. Romberg, C. Oussoren, C.J. Snel, M.G. Carstens, W.E. Hennink, G. Storm, Biochim. Biophys. Acta Biomembr. 1768 (2007) 737.
[39] H.-M. Yang, H.J. Lee, K.-S. Jang, C.W. Park, H.W. Yang, W.D. Heo, J.-D. Kim, J. Mater. Chem. 19 (2009) 4566.
[40] H.-M. Yang, C.W. Park, M.-A. Woo, M.I. Kim, Y.M. Jo, H.G. Park, J.-D. Kim, Biomacromolecules 11 (2010) 2866.
[41] H.J. Lee, K.-S. Jang, S. Jang, J.W. Kim, H.-M. Yang, Y.Y. Jeong, J.-D. Kim, Chem. Commun. 46 (2010) 3559.
[42] H. Chen, T. Chen, J. Hu, C. Wang, Colloids Surf. A. Physicochem. Eng. Aspects 268 (2005) 224–268.
[43] M. Rohrer, H. Bauer, J. Mintorovitch, M. Requardt, H. Weinmann, J. Invest. Radiol. 40 (2005) 715.
[44] E. Okon, D. Pouliquen, P. Okon, Z.V. Kovaleva, T.P. Stepanova, S.G. Lavit, B.N. Kudryavtsev, P. Jallet, Lab. Invest. 91 (1994) 895.
[45] K.J. Tapan, K.R. Maram, A.M. Marco, L.L.-P. Diandra, L. Vinod, Mol. Pharm. 5 (2) (2008) 316.
[46] K. Briley-Saebo, A. Bjornerud, D. Grant, H. Ahlstrom, T. Berg, G.M. Kindberg, Cell Tissue Res. 316 (2004) 315.